JOURNAL OF GEOPHYSICAL RESEARCH, VOL. 90, NO. B13, PAGES 11,294–11,302, NOVEMBER 10, 1985

"Slow" Physics of Large Continental Ice Sheets and Underlying Bedrock and Its Relation to the Pleistocene Ice Ages

G. EDWARD BIRCHFIELD AND ROBERT W. GRUMBINE

Department of Geological Sciences and Department of Engineering Sciences and Applied Mathematics
Northwestern University, Evanston, Illinois

Very simple two-component models of the earth's cryosphere-lithosphere system are analyzed. The models consist of a continental ice sheet coupled to a responding earth model. Because of relatively long response times of the bedrock, at least over shorter wavelengths, long-period (of the order of 50,000 years) internal or "free" oscillations in the system occur over a wide range of parameters and parameterizations. The oscillatory mechanism operates primarily in the ablation zone and in particular at the firn line. These free oscillations could play a dynamic role in the response of the climate system to eccentricity forcing. A simple analysis presented strongly suggests that for the simplest rheological models of the earth response to Pleistocence ice sheets, elastic response is confined to a layer considerably less than the thermal thickness of the lithosphere. Furthermore, because of the striking lack of geological evidence for large depressions of bedrock at the leading edge of growing continental ice sheets, predicted by viscoelastic models of the earth, more sophisticated rheological models of the earth's uppermost layer appear necessary.

1. INTRODUCTION

Observational evidence from deep-sea sediments over the last few years has built an increasingly clear picture of the many alternating glaciations and interglacials of the Pleistocene. A major source of this information on the changing ice volumes has been oxygen 18 stable isotope analyses of planktonic and benthic formaminefera shells deposited in the deep-sea sediments. Although these isotope records reflect the combined effect of water temperature and water isotope values, it is generally accepted that the latter changes dominate the signal, allowing the record to be viewed as a first approximation to continental ice volume changes (see, for example, *Broecker and Van Donk* [1970], *Shackleton and Opdyke* [1973], and *Imbrie et al.* [1984]). The ice volume record appears to show several distinctive phases over the last two million years; the most well documented and distinctive phase appears in the late Pleistocene, that is, for the last several hundred thousand years. Here the ice volume changes appear to be considerably larger than earlier; they are remarkably regular, with glacials persisting for approximately 10^5 years, separated by relatively brief interglacials.

Considerable progress has been made in understanding the causes of the Pleistocene Ice Ages. *Hays et al.* [1976] have shown that the spectral properties of the time series of changes of insolation received in high northern hemisphere latitudes caused by perturbations of the eccentricity, the obliquity, and the precession of the longitude of perihelion of the orbit of the earth compare well with those of the ice volume record for the late Pleistocene. The most prominent peaks in the orbital spectra associated with the precession of longitude of perihelion and with the obliquity correlate well with peaks appearing in the ice volume record; reasonable phase lags of a few thousand years between the former and the latter also are found.

The comparison of the ice volume record with the changes in eccentricity is not as simple. The spectral analysis of the eccentricity changes themselves shows prominent signals near 100,000 years and near 400,000 years. But because of the very small eccentricity changes, insolation changes at these periods are quite small. The spectral analysis of the isotope series, however, has the most prominent response near 100,000 years. *Hays et al.* [1976] pointed out that it is likely that this response is essentially nonlinear.

Several models have been proposed with different nonlinear mechanisms to account for the response at 100,000 years. Most prominent are those of Saltzman (see, e.g., *Saltzman et al.* [1985]) and Ghil (see, e.g., *Le Treut and Ghil* [1983]). These models have in common, first, the explicit inclusion of at least two components of the climate system, one of which is the atmosphere, second, a formulation that is in terms of globally averaged dependent variables, the resulting model equations being coupled nonlinear ordinary differential equations. One important mechanism is the nonlinear generation of combination tones from the precessional forcing at 19,000 years and 23,000 years. This has also been discussed by *Wigley* [1976], *Birchfield* [1977], and *Birchfield et al.* [1981]. Focus has also been on possible existence in the multicomponent climate system of coupled feedback mechanisms capable of producing internal or self-sustained oscillations; such oscillations if of sufficiently long period, might produce a resonant response to the weak eccentricity forcing, or if of shorter period, generate a long-period response through combination tones.

We approach the question of mechanisms responsible for the response at 100,000 years for the late Pleistocene by examining the "slow physics" of the large continental ice sheets and the underlying earth as it responds to the varying ice load. Very simple numerical models have been studied with a focus on possible periodic responses. These models differ from the above in that the "fast" processes in the atmosphere are bypassed; they are, in addition, spatially dependent, with model equations being partial differential equations with many degrees of freedom. It is found that this "two-component" system manifests self-sustained oscillations of periods of the order of 50,000 years over a wide range of parameters and model variations. The mechanism responsible for these oscillations is discussed and possible roles of the slow physics in the 10^5-year climate record are considered.

Paper number 4B5417.
0148-0227/85/004B-5417$05.00

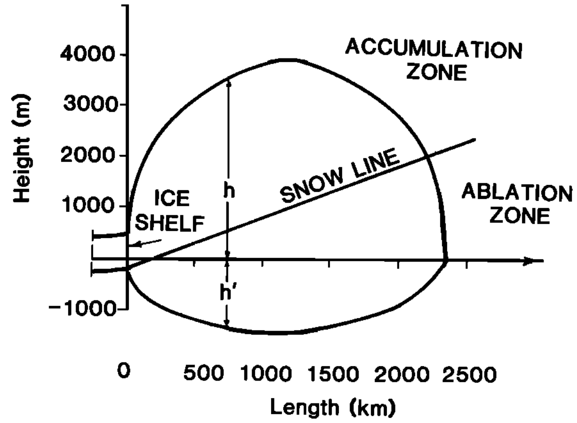

Fig. 1. A schematic picture of a cross section of the model ice sheet.

2. MODEL DESCRIPTION

The physical basis for the ice sheet model we have used has been described by *Birchfield et al.* [1981]. The two-dimensional model features are shown schematically in Figure 1. The ice sheet is bounded on the north by a polar ocean; the continent extends indefinitely to the south with no topography. An ice shelf is assumed to exist poleward of the continent when an ice sheet is present. The boundary condition for the ice sheet at the junction with the ice shelf is simply to limit the free surface elevation to a prescribed maximum elevation (usually taken as 400 m) or to set the slope of the ice sheet to zero, for elevations less than the limit. There is little direct justification for this boundary condition other than its utility in avoiding modeling of the marine ice component and the fact that the observed elevation at the edge of present-day ice sheets is of the order of a few hundred meters. A more realistic treatment of the boundary may make significant alterations in the model response but must be deferred to subsequent experiments.

The equation for ice mass conservation is

$$\frac{\partial h}{\partial t} + \frac{\partial M}{\partial x} = A - \frac{\partial h'}{\partial t} \tag{1}$$

$$M \equiv -\lambda H^5 \left(\frac{\partial h}{\partial x}\right)^3 \qquad H \equiv h + h' \tag{2}$$

where h is the elevation of the ice surface above sea level, h' is the elevation of bedrock below sea level, t is time M is the horizontal flux of ice per unit width of the ice sheet, and λ is a flow law constant. The λ has been adjusted to crudely allow for basal sliding (see *Birchfield et al.* [1981] for a detailed derivation of this parameter).

The snowline intersects sea level $x_0(t)$ km from the polar ocean. The mean annual accumulation rate $A(x, t)$ is based on a "temperature" field increasing linearly southward and with decreasing elevation z:

$$T = \gamma[s(x - x_0) - z]$$

where γ is the lapse rate and s the slope of the "isotherms." The very greatly simplified accumulation rate is taken to be

$$\begin{aligned} A &= a[1 + bT] & T &\le 0 \\ A &= -a - \alpha b_1 T & T &> 0 \end{aligned} \tag{3}$$

where a, b, b_1, and α are constants. Values for the constants in the ice sheet component are shown in Table 1. The accumulation rate thus decreases with increasing elevation and with increasing latitude. This incorporation of the moving snow line x_0, varying with time, and the spatially varying and time-varying accumulation rate A represents the parameterization of the entire response of the hydrological cycle and the atmosphere to the perturbations of solar radiation resulting from orbital fluctuations.

TABLE 1. Values of Constants Used in the Ice Sheet Component Model

Satellite	Typical Value
λ	$1.42286E - 12$ m^{-3} s^{-1}
γ	0.008 k^{-1} m^{-1}
s	$1.0\ E - 3$
a	1.2 m a^{-1}
b	0.0166 k^{-1}
b_1	0.635 m a^{-1} k^{-1}
α	0.4

Two models of bedrock response to the time-varying ice load have been used. The first is extremely simple and is identical to that used by *Birchfield et al.* [1981]. This model assumes that (1) at each point under the ice sheet only the ice load at that point and its history affect the bedrock displacement at that point and (2) the bedrock has a single response time τ independent of the size of the ice sheet. This model amounts to using only one single spatial harmonic function with a horizontal half wavelength corresponding to a mean ice sheet size, in a one-layer homogeneous incompressible viscious layer model of the earth, neglecting sphericity and gravity variations.

The second bedrock model assumes again a flat earth, and constant gravity; it consists of an upper perfectly elastic lithosphere of depth D, of constant density ρ_L, and elastic rigidity μ, overlying a viscous asthenosphere of unbounded depth, density ρ_A, and viscosity η. Here the equations are expanded in Fourier series in x and solved by means similar to those of *Cathles* [1975] for the downward displacement $h'(x, t)$ of the earth's surface under the varying ice load. In this model the relaxation time for the ice sheet varies with wavelength and will be discussed in the next section. The details of the derivation of the model equations are given in Appendix A. Values taken for the constants in the earth model are tabulated in Table 2.

The method of numerical solution of (1), (2), and the bedrock displacement equations (A1) is critical to the results we have obtained. A good deal of attention in particular has been given to the solution of (1); this equation is nonlinear in h not only through the mass flux divergence term but also through the dependence of the accumulation rate on the elevation and shape of the ice sheet. The lack of consistent evidence from

TABLE 2. Values Used for Constants in the Earth-Component Model

Constant	Typical Value
D	40 km
ρ_L	3000 kg m^{-3}
μ	10^{11} Pa
ρ_A	3800 kg m^{-3}
η	10^{21} Pa s

Birchfield and Weertman [1984] of the response described here was due to inadequate understanding of some aspects of the numerical model. A brief summary of the numerical procedure is presented here with further discussion in Appendix B.

For one time step: Starting from initial spatial values of ice sheet elevation h and bedrock depression h', the spectral coefficients H_l are computed for the ice sheet thickness H. The spectral equations for bedrock displacement coefficients h_l (equations A1) are extrapolated, to yield, after taking their inverse transform, the bedrock displacement for the next time step. After calculating the accumulation rate over the entire ice sheet grid using (3), (1) is integrated using a generalized Newton-Raphson finite-difference method to yield the surface elevation h of the ice sheet at the new time step.

Critical elements in the numerical solution are (1) a sufficiently small spatial grid spacing (20 km) and the corresponding small time step (20 years), (2) an accurate determination of the position of the firn line, used in calculating the accumulation rate, and (3) accurate numerical methods for calculating mass flux at the leading edge and polar boundary of the ice sheet. (These are needed even though the underlying physics in these regions is not accurate, for example, due to the neglect of normal stresses and ice shelf coupling.)

3. Lithospheric Thickness for the Two-Layer Earth Model

The composition and physics of the oceanic lithosphere are considerably better understood than those of the lithosphere underlying the continents. The "thermal" definition, based on the depth of the solidus temperature, implies increasing thickness away from the mid-ocean ridges, with thickness of "old" lithosphere near 100 km [*Turcotte and Schubert*, 1982]. The "elastic" definition of thickness, based on the temperature at which elastic stresses are relaxed by solid state creep, yields depths approximately one half those of the thermal depth; these depths estimated from rheological models are reasonably well supported, for example, by studies of focal depths of intraplate earthquakes [*Turcotte and Schubert*, 1982; *Chen and Molnar*, 1983; *Wiens and Stein*, 1983].

The situation for the continental lithosphere is not so clear. For global purposes where little distinction is made between oceanic and continental lithosphere, values range from 70 to 120 km (see, for example, *Uyeda* [1978]), with a typical value being 100 km. Whereas the composition of the oceanic lithosphere is pretty much accepted, the composition of the lower lithosphere under the continents is not. *Sibson* [1982] and *Chen and Molnar* [1983] have made estimates of ductile strength of continental lithosphere for different rock compositions. Their results suggest that the continental lithosphere may have somewhat lower strength than oceanic lithosphere; their conclusion and also that of *Wiens and Stein* [1983] is that the elastic depth may be somewhat less under the continents than under the oceans.

The (temperature) depth at which elastic stresses are relaxed depends, of course, on the length of time for which the stresses have been applied. It is not clear as to what load times are implicit in the studies of the depths of earthquake foci, but most likely they are longer than characteristic load times for the Pleistocene ice sheets. We have estimated the stress relaxation depth (temperature) using the approximate rheological analysis of *Turcotte and Schubert* [1982, chapter 7.10] for several rocks which may be representative of the continental lithosphere, for load times of 10^4 to 10^5 years and stresses of 12 mPa, characteristic of large continental ice sheets (see, for

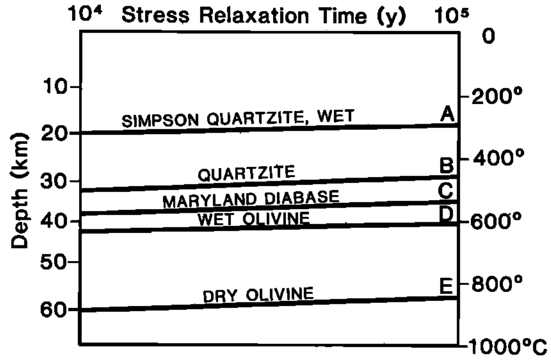

Fig. 2. Estimated stress relaxation time, defined as time required for stress to fall to half of its initial value, versus depth and temperature in lithosphere. This is computed from the rheological law for a Maxwell solid, assuming a stress dependent effective viscosity; a rearranged (7-248) [*Turcotte and Schubert*, 1982] is used. Rheological and thermodynamical data are given from *Clark* [1966] and for A from *Sibson* [1982], B and C from *Chen and Molnar* [1983], and D and E *Turcotte and Schubert* [1982].

example, *Weertman* [1978]). From the results shown in Figure 2 we have chosen the thickness of the perfectly elastic upper layer in our two-layer model, $D = 40$ km, for the majority of the numerical experiments; however, the overall range of depths investigated ranged from 5 to 120 km.

4. Numerical Experiments With the Simple Bedrock Model

The objectives were to obtain a greatly simplified two-dimensional numerical model of large continental ice sheets, (1) which given the surface accumulation rate as a function of time, predicts changes in the volume on the time scale of the Pleistocene ice sheets, (2) which is suitable for incorporation into a paleoclimate model containing atmosphere, surface and deep ocean components, (3) which is adequate to investigate the role of feedback mechanisms between the earth bedrock and the changing ice load, (4) in particular, which could clarify the role of these two elements of the slow physics of the climate system of the earth in producing the 100,000-year oscillations. The models presented are, of course, suitable for incorporating into more general climate models.

The initial development of the numerical ice sheet model was done with the older version of bedrock physics. For many experiments in which the snow line was held fixed in time, once mass balance was reached, it did not remain in equilibrium; the ice volume displayed oscillations in these instances with a period of 30,000–60,000 years; the range in volume changes was as large as 50% of the maximum equilibrium volume. The model was clearly displaying self-sustained oscillations.

The mechanism responsible for the oscillation can be described qualitatively. When the ice volume first reaches equilibrium, the underlying bedrock has not completely adjusted to the ice load in the region extending from the firn line to the leading edge; that is, the bedrock is still sinking with consequent lowering of the upper surface of the ice sheet in this region.

The lowering of the surface of the ice sheet in the ablation zone has two effects both acting with positive feedback: First, the ablation rate will increase with decreasing surface elevation, from (3). Until changes in horizontal mass flux can be effected, there is less of a drop and hence less change in the accumulation zone.

Secondly, and more importantly, a drop in the ice sheet elevation at the firn line results in its northward displacement, that is, an increase in the dimensions of the ablation zone; for example, a drop of surface elevation of 20 m at the firn line displaces the line 20 km poleward; the accumulation zone area is reduced by an equal amount. Since at the initiation of a collapse cycle the ice sheet is in mass balance, both halves of the ice sheet are separately in balance; thus in the early stages of collapse, only the southern half of the ice sheet is involved, and the decrease in accumulation zone width is percentagewise relatively large. Thus the initial decrease in ice volume can be quite rapid.

The negative mass balance is eventually reversed by two effects. First, because of increased mean slope on the south side of the ice sheet resulting from increased ablation at the southern extremity of the ice sheet, there is an increasing southward mass flux supplied from the north side of the ice sheet; this results in a poleward and downward shift of the ice dome. With this shift there is an increasing width of the accumulation zone on the south side of the ice sheet and an increase in the accumulation rate, the latter effect being partially compensated by the poleward gradient in accumulation rate.

Second, with the retreat of the ice sheet leading edge northward toward the fixed sea level snow line position, the width of the ablation zone decreases, tending to reduce the total ablation. Also, the increase in ablation caused by the decrease in the mean elevation of the ablation zone tends to be compensated by the decrease due to the northward shift of the ablation zone. When these processes come into play, the ice sheet regrows toward its initial mass balance along a path similar to its original path.

5. EXPERIMENTS WITH THE TWO-LAYER EARTH MODEL

While very simple, the two-layer model goes beyond the single-layer model, representing at least in a rudimentary way the effects of elastic behavior of the surface layer of the earth. It lacks, of course, the more complex structure of the deeper mantle, which *Peltier* [1982] and others have shown to be necessary to explain the gravity anomalies persisting in the locations of the former Laurentide and Fennoscandian ice sheets.

From experiments with the two-layer model incorporated into the ice sheet model we encounter what we believe to be a serious limitation of all such models which have a simple elastic surface layer. *Hughes* [1981] has forcefully presented essentially the same argument. During ice sheet growth a trough develops extending several hundred km ahead of the ice sheet and more than 200 m deep at the leading edge of the ice sheet. During ice sheet retreat, the trough persists, but with a slowly decaying bulge appearing farther out with an elevation some tens of meters above sea level. A great deal of research has been concerned with the question of existence of the forebulge after the time of the last glacial maximum. Evidence at this time primarily from the eastern seaboard does support its existence; see, for example, *Cathles* [1975, chapter 4] and *Peltier* [1982].

While there also exists a great deal of evidence of large proglacial lakes during the retreat stages of the Wisconsinin, we have found no literature which presents geological evidence of the existence of such large depressions at the leading edge of the ice sheet during its growth or at the time of maximum extent. Flint's map of glacial reconstruction [*Flint et al.*, 1959] does not show large proglacial lakes at the time of maximum extent. It is difficult to incorporate the presence of such a deep trough in a consistent way into *Flint*'s [1971] discussion of the hydrology of the region south of the Laurentide ice sheet maximum. *Daly* [1974] notes lack of evidence of both forebulge and depression ahead of the ice sheet. *Hughes* [1981], in noting the absence of geological evidence of large depressions, investigates the effect of elastic-plastic rheology as a possible alternative.

It can be argued that at its maximum the last ice sheet was shallow over the region near its leading edge and hence no large depression would be present. To test this with the two-layer earth model, we artificially reduced the ice thickness several grid points behind the leading edge and found virtually no alteration in the bedrock depression ahead of the ice sheet; the depression is controlled by the large-scale properties of the ice sheet load and not the load at the leading edge.

As might be expected, in the two-layer model experiments, the presence of a large depression ahead of the growing ice sheet tends to either eliminate the "equilibrium" oscillations occurring in the single-layer earth model or reduce significantly their amplitude. In order to achieve an earth response ahead of the ice sheet that is more consistent with the evidence, we have made a crude alteration in the two-layer model response ahead of the ice sheet. In this region we assume no depression until the ice sheet arrives; south of a retreating ice sheet, bedrock response is calculated using the simple adjustment model described in the previous section. Most of the experiments discussed in the following have been made with this alteration in bedrock response ahead of the ice sheet.

6. ROBUSTNESS OF THE MODEL OSCILLATORY RESPONSE

We have taken considerable pains to establish the "robustness" of the self-sustained oscillations observed in our two-component paleoclimate model. Unless specified otherwise, parameters used in experiments are those given in Tables 1 and 2. Experiments have been made for a wide range of initial conditions; in Figure 3 the initial ice volume was chosen close to equilibrium, but with bedrock depression not near equilibrium. The oscillations become regular after the first cycle with a period of approximately 52,000 years and a range of about 25% of the maximum ice volume. If the same experiment is made with bedrock initially close to the steady state solution, the oscillatory response does not appear (Figure 3).

Oscillations occur over a wide range of model lithosphere thicknesses. The thicker the lithosphere, the larger the ice sheet required for oscillatory response; for a thickness of $D = 5$ km, oscillations occur for an ice sheet width as small as $L = 1700$ km; for $D = 80$ km, they occur with $L = 3800$ km. Figure 4 shows a cross section of an ice sheet during the collapse part of the cycle; D has been chosen small to dramatize the response.

A sensitive control is the difference in density of ice and the asthenosphere which controls the maximum sinking of the bedrock. For an asthenosphere of density 3500 kg m^{-3} the volume oscillatory range is 3.3×10^9 m^2, the period 47,000 years; if the density is taken as 4500 kg m^{-3}, then the range is 1.3×10^9 m^2, period 63,000 years. For standard parameters, if the density is 5000 kg m^{-3}, oscillations do not appear.

As seen in Figure 3, oscillatory response can occur when the snow line at sea level is well north of the continent. Figure 5 is a plot of equilibrium ice volume versus position of the sea level snow line with respect to the contitnent edge. For this particular example, oscillations disappear when $x_0 = 550$ km.

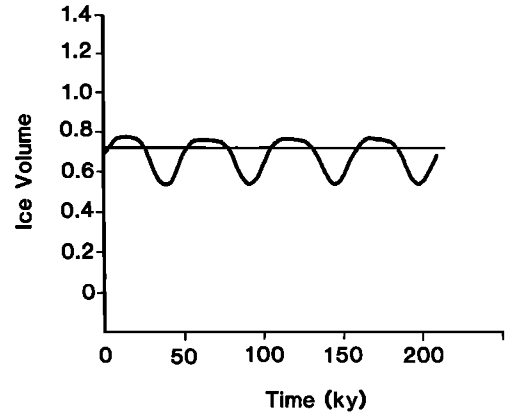

Fig. 3. Self-sustained oscillations starting from a large ice sheet which is in near mass balance but in which the bedrock is not in equilibrium with the ice load. The steady state response curve is for mass balance with bedrock equilibrium initial conditions.

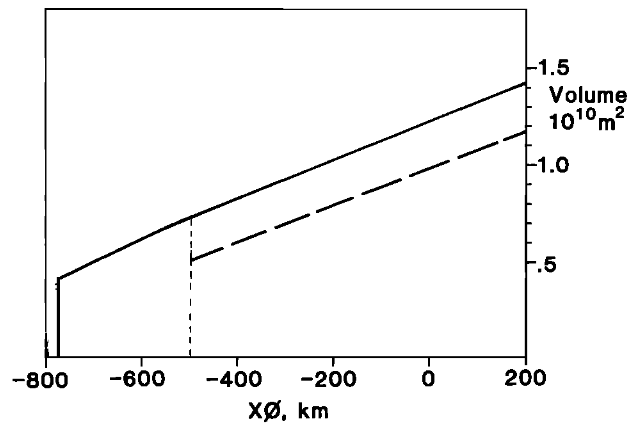

Fig. 5. Equilibrium response of the model versus sea level position of the snowline. For $x_0 >$ circa 550 km, the ice volume oscillates between the upper solid curve and the lower dashed curve; for $-775 < x_0 < -550$ km a steady state solution exists as shown by the continuation of the solid line. In addition, a steady state solution of zero ice volume exists for all negative x_0.

Stable nonzero ice sheet nonoscillating solutions disappear when the snow line is more than 775 km north of the edge of the continent.

Figure 6 shows a typical profile of the relaxation time for the external mode of the earth model versus wavelength of the ice loading. (An ice sheet of, say, 2000 km extent has the largest contribution to the load at a wavelength of 4000 km.) This response is very close to that of the external mode in *Peltier*'s [1982] model. The distinctive feature is that relaxation times decrease for both small- and long-wavelength loads, the former due to the presence of the elastic lithosphere, the latter to the deep viscous asthenosphere.

For a large ice sheet the relaxation time for the major load contribution is rapid, i.e., in wavelengths well to the right of the peak. Bedrock response to the expansion of the southern region of the ice sheet will involve significant changes in the amplitudes of much shorter wavelengths closer to the wavelength of maximum relaxation time, and hence a slower response to the ice load under the ablation zone of the ice sheet should result. The wavelength of maximum relaxation time and its value changes for different model parameters, but the response does not appear to be sensitively related to these properties of the relaxation spectrum.

Various values of the constants in the accumulation rate have been tested. Different formulations of the accumulation rate calculation have also been tested with no significant alteration of the response.

7. General Discussion

It is indeed an important question in the validation of the astronomical theory to understand the source or sources in the climate system which produce the prominent response near 100,000 years. Although there may be an important temperature contribution to the stable isotope record in the late Pleistocene, it is certainly smaller than that from ice volume changes; it is unlikely that all of the power at 100,000 years comes from the temperature signal. *Imbrie et al.* [1984] have shown significant correlations in the spectral domain between eccentricity variations near 100,000 years and the signal in the isotope record and that the phase relation at that period is consistent with a resonance phenomenon. Although their spectral analysis was done on time series of the geological record which themselves had been tuned to insolation

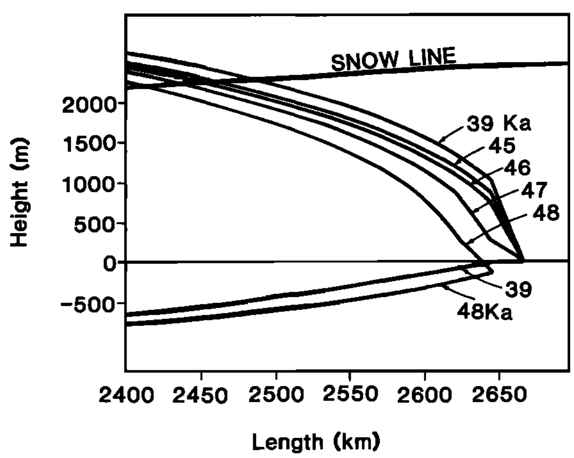

Fig. 4. Collapse of a large ice sheet initially in near mass balance, resulting from sinking of the upper surface due to bedrock sinking subsequent to the time mass balance was reached.

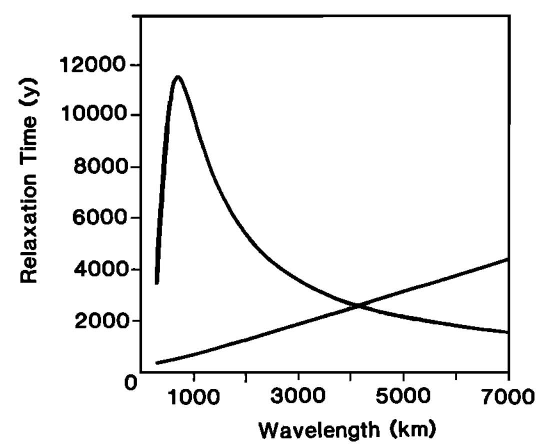

Fig. 6. Relaxation time of the modes for the two-layer earth model versus horizontal wavelength. The amplitude of the response for the internal mode, i.e., the monotonic curve, is very much smaller than that for the external mode, i.e., the bell-shaped curve.

changes, the tuning process involved only those periods associated with changes in the earth's obliquity and precessional parameters, i.e., at 41 and 22 ka. This evidence then strongly suggests that the response at 100,000 years is indeed related to the astronomical forcing.

Kallen et al. [1979], *Ghil and LeTreut* [1981], *LeTreut and Ghil* [1983] and *Saltzman et al.* [1981, 1982] have identified nonlinear mechanisms in two- and three-component climate models which can produce self-oscillations of relatively short periods, circa 3000 years for the latter group and 10,000 years for the former. They demonstrate, however, that the presence of these "free" oscillations can, with external forcing, via combination tones, produce large response near 100,000 years. The period of the free oscillations is relatively small because their components involve the relatively fast responding elements of the climate system, e.g., the atmosphere, surface ocean, sea ice, and the deep ocean. More recently, *Saltzman and Sutera* [1984] and *Saltzman et al.* [1984] present three-component models incorporating a crude representation of the retardation effect of marine ice shelves as a slow process which show free oscillations near 100,000 years.

With a model incorporating only slow physics elements, *Oerlemans* [1982] identifies a basal melting feedback with ice sheet physics to produce internal oscillations near 100,000 years. *Pollard* [1984] couples slow physics processes: a feedback mechanism between formation of proglacial lakes, ice sheet physics, and bed rock sinking to a simple atmospheric model; under control of the slow processes, 10^5-year cycles are prominently displayed. *Pollard* [1983] has also followed a somewhat similar procedure in a marine context producing interaction between ice sheet, bedrock, and sea level which also results in long-period oscillations.

Oerlemans [1982] and *Birchfield et al.* [1981] have investigated two-component models comprising feedback between bedrock sinking and ice sheet physics only; their representation of bedrock sinking physics is essentially the same as that of the simple earth model presented here. In the former, with simple periodic forcing experiments, large 100,000-year oscillations are achieved only by taking unrealistically long relaxation times for bedrock sinking. In the latter, using a relaxation time of 3,000 years and using *Berger*'s [1978] coefficients for insolation perturbations, a fairly good reproduction of the ice volume record was achieved; the power at 100,000 years produced nonlinearly, i.e., through combination tones, by the precessional forcing at 19,000 and 23,000 years was considerably smaller than the spectra of the isotope records would suggest, however.

Peltier and Hyde [1984] have simplified *Peltier*'s [1982] multilayered viscoelastic earth model by taking only the external mode of response and integrating this with an ice sheet model similar to that of *Birchfield et al.* [1981]. His earth model includes the sphericity of the earth, but his ice sheet is two dimensional. When this model is forced at 20,000 years, a strong response appears at 20,000, 40,000, 60,000, 80,000, and 100,000 years, with the largest amplitude at 100,000 years. We have seen no evidence of such a phenomenon in our model with preliminary testing. Although there are differences between our model and theirs, it is primarily in the method of numerical solution. This is being pursued further.

The mechanism for the self-sustained oscillations discussed herein should be present in most of the models discussed above but not in *Birchfield et al.*'s [1981] because of the fast response time of the bedrock. This possibility was first pointed out by *Peltier* [1982]. The fact that they are so apparent in the present model, we believe, is due to the improved method of numerical integration. Although their presence does not require a very sophisticated earth model, it does require relatively long relaxation times over some part of the spatial spectrum; even with the long relaxation times of the bedrock confined to short wavelengths, the sinking of the surface of the ice sheet near the firn line can be sufficient to cause the ice sheet to collapse relatively far out of mass balance, which, when coupled with restorative processes, produces an oscillatory response.

The period of the internal oscillations in no experiment yet run has approached 10^5 years in length. The most common period is slightly greater than 50,000 years. The presence of robust free oscillations at this period produced by such a simple mechanism in the slow physics is encouraging, however. The work of Ghil and Saltzman referred to above and that of *Nicolis* [1984], although focusing on the fast physics components, demonstrates clearly the potential "usefulness" of such a free oscillation in the response to the astronomical forcing. Such long-period free oscillations have the advantage that they are much closer to the dominant period and hence favor the eccentricity-forcing possibility.

An additional intriguing aspect of the eccentricity forcing problem has been presented by *Imbrie* [1985]. In addition to the small eccentricity forcing components near 100,000 years, there is an even smaller component at 59,000 years; *Imbrie* [1985] reports that there is a similar period in the proxy ice volume data and that this signal is statistically coherent with the very small eccentricity forcing. His statistical analysis shows further that the climate system appears most sensitive to the astronomical forcing in this part of the spectrum. If this is not a subtle effect of the tuning procedure used in constructing the stacked record, is it possible that a mechanism of resonance, such as the one proposed here, can enhance a signal even though it is in the "noise" level of the record?

8. CONCLUSIONS

We are in the process of introducing simple periodic forcing into the model as a prelude to the astronomical forcing. From the results of the study so far we summarize and conclude as follows:

1. There exists in very simple ice sheet–bedrock models an internal oscillation mechanism. This mechansim operates in the most rapidly changing section of the ice sheet, here in the southern ablation zone and under the firn line.

2. The internal oscillations are robust to a wide range of parameters and for different parameterizations; they are sensitive to firn line perturbations and in both amplitude and period to the spatial gradient in the accumulation rate; the elastic lithosphere acts as a low pass filter: The greater the depth of the lithosphere, the larger the ice sheet dimensions required for the mechanism to be active.

3. The presence of free oscillations, whether long or short period, in the earth's climate may play a dynamic role in the response of the system to the astronomical forcing; long periods could particularly favor the eccentricity forcing.

4. A simple analysis strongly suggests that for simplest rheological models of the bedrock response to ice sheet loading on the time scale of the Pleistocene ice sheets, elastic response is confined to a layer considerably less than the thermal thickness of the lithosphere.

5. Because viscoelastic rheologies for the earth give large bedrock sinking at the leading edge of a growing ice sheet for which there is a striking lack of geological evidence, a more

sophisticated rheology, perhaps along the lines suggested by *Hughes* [1981], is required.

APPENDIX A: THE TWO-LAYER EARTH MODEL EQUATIONS

The equations of motion for the perfectly elastic lithosphere are the following:

$$\frac{\partial \tau_{xx}}{\partial x} + \frac{\partial \tau_{xz}}{\partial z} - \rho_L g \frac{\partial w}{\partial x} = 0 \qquad \tau_{xx} \equiv 2\mu \frac{\partial u}{\partial x}$$

$$\frac{\partial \tau_{zx}}{\partial x} + \frac{\partial \tau_{zz}}{\partial z} - \rho_L g \frac{\partial w}{\partial z} = 0 \qquad \tau_{zz} \equiv 2\mu \frac{\partial w}{\partial z}$$

$$\frac{\partial u}{\partial x} + \frac{\partial w}{\partial z} = 0 \qquad \tau_{xz} \equiv \mu\left(\frac{\partial u}{\partial z} + \frac{\partial w}{\partial x}\right)$$

where τ_{xx} and τ_{zz} are the normal stresses and τ_{zx} is the shear stress; u and w are the horizontal and vertical displacements, μ is the rigidity, and ρ_L is the density. The boundary conditions at the surface $z = 0$ are taken to be

$$\tau_{zx} = 0 \qquad \tau_{zz} = -\rho_I g H(x, t)$$

where ρ_I is the density of the ice. The equations of motion for the asthenosphere are

$$\frac{\partial \tau_{xx}}{\partial x} + \frac{\partial \tau_{xz}}{\partial z} = 0 \qquad \tau_{xx} \equiv 2\eta \frac{\partial \dot{u}}{\partial x}$$

$$\frac{\partial \tau_{zx}}{\partial x} + \frac{\partial \tau_{zz}}{\partial z} = 0 \qquad \tau_{zz} \equiv 2\eta \frac{\partial \dot{w}}{z}$$

$$\frac{\partial \dot{u}}{\partial x} + \frac{\partial \dot{w}}{\partial z} = 0 \qquad \tau_{zx} \equiv \eta\left(\frac{\partial \dot{u}}{\partial z} + \frac{\partial \dot{w}}{\partial x}\right)$$

where η is the viscosity coefficient and the dot denotes differentiation with respect to time t. At the interface with the lithosphere, in addition to having continuous displacements, shear stress, and x component of the normal stress across the interface for all time, the z-normal stress noundary condition must include a buoyancy term:

$$Z = -D \qquad (\tau_{zz})_{\mathrm{LITH}} = (\tau_{zz})_{\mathrm{ASTH}} + \rho_A g w$$

where ρ_A is the uniform density of the asthenosphere and w the vertical displacement of the lithosphere-asthenosphere interface.

Instead of taking continuous Fourier transforms as in the work by *Cathles* [1975], we expand the solutions in the two layers in Fourier series over the domain

$$-\Delta x - L \le x \le L$$

where L is the length of the ice sheet grid plus Δx, the grid finite difference interval. This expansion over the interval is in effect an imposition of periodicity boundary conditions over this wavelength and an odd extension. The earth then senses repeated ice sheets spaced at this interval, instead of a single ice sheet. If the region significantly affected by the ice load is well inside the interval, this representation should be no worse than the flat earth approximation already invoked.

The expansions in the upper layer are, for example,

$$H(x, t) = \sum_{l=0}^{N} H_l(t) e^{ik_l(x-\Delta x)}$$

$$u(x, t) = \sum_{l=0}^{N} u_l(z, t) e^{ik_l(x-\Delta x)} \qquad k_l \equiv 2\pi l/L$$

$$w(x, z, t) = \sum_{l=0}^{N} w_l(z, t) e^{ik_l(x-\Delta x)}$$

where N is the number of grid intervals on the ice sheet grid.

The expansions are substituted into the equations for the two layers and, using the orthogonal properties, reduced to equations for the Fourier coefficients of the variables. These consist of a system of first-order differential equations in z and are reduced to Runge-Kutta form (see Appendix 2 of *Cathles* [1975]). Solving these and imposing boundary conditions at the interface and at the surface, the following equations for the surface displacements are found for each wavenumber l, after considerable reduction:

$$\frac{dx_l}{dt} = A^l x_l + H_l E^l + \dot{H}_l F^l$$

$$A^l \equiv a_{ij}{}^l \qquad E^l \equiv e_i{}^l \qquad F^l \equiv f_i{}^l \qquad x_l \equiv a_i{}^l$$

$$a_{11}{}^l \equiv \frac{-\mu}{\eta}\left[\frac{shv chv + v + \delta\varepsilon ch^2 v}{ch^2 v + v^2}\right]_l$$

$$a_{12}{}^l = \frac{\mu}{\eta}\left[\frac{v^2 - \delta\varepsilon chv(chv - vshv)}{ch^2 v + v^2}\right]_l$$

$$a_{21}{}^l = \frac{\mu}{\eta}\left[\frac{v^2 - \delta\varepsilon chv(chv + vshv)}{ch^2 v + v^2}\right]_l$$

$$a_{22}{}^l = -\frac{\mu}{\eta}\left[\frac{shvchv - v + \varepsilon v^{-1}(ch^2 v - v^2 sh^2 v) + vch^2 v\varepsilon_1}{ch^2 v + v^2}\right]_l \qquad \text{(A1)}$$

$$e_1{}^l = -\frac{\mu}{\eta}\left[\frac{vchv(shv - vchv)}{ch^2 v + v^2}\right]_l \delta\varepsilon\rho_I g$$

$$e_2{}^l = \frac{-\mu}{\eta}\left[\frac{ch^2 v + v^2 + [(1 - v^2)shvchv - v]\delta\varepsilon}{ch^2 v + v^2}\right]_l$$

$$f_1{}^l = \left[\frac{v^2}{ch^2 v + v^2}\right]_l \rho_I g \qquad f_2{}^l = \left[\frac{v - shvchv}{ch^2 v + v^2}\right]_l \rho_I g$$

$$a_1{}^l = 2\mu i k_l u_l(0, t) \qquad a_2{}^l = 2\mu k_l w_l(0, t)$$

$$h_l'(t) = -w_l(0, t) = \frac{-a_2{}^l}{2\mu k_l}$$

$$\varepsilon = \frac{\rho_A g D}{2\mu} \qquad \varepsilon_1 = \frac{\rho_L g D}{2\mu} \qquad \delta\varepsilon = \varepsilon - \varepsilon_1$$

$$chv \equiv \cosh v \qquad shv \equiv \sinh v$$

$$v \equiv v_l \equiv k_l D$$

where $h_l'(t)$ is the Fourier component of bedrock sinking.

The elastic contribution to the surface displacement is small, and the loading terms involving the time derivative of H_1 may be neglected in (A1). As in the multilayer models of *Peltier* [1982], there is more than one mode of response to surface loading for each spatial wave number; for our two-layer model there is an external mode associated with the upper surface of the lithosphere and an internal mode arising from the presence of the boundary between the lithosphere and the asthenosphere. The contribution to the surface response from the internal mode appears to be quite small and probably could be safely neglected, which would result in considerable simplification of (A1). (*Peltier* [1982] has neglected all internal modes.) Because of the two modes of response there are two sets of relaxation times, one for each mode. The relaxation times can be easily found by solving for the characteristic values of the matrix a_{ij}^{l}. We have solved (A1) by straightforward numerical integration as discussed in Appendix B.

APPENDIX B. NUMERICAL INTEGRATION OF THE ICE SHEET–BEDROCK MODEL

An implicit finite difference scheme is used to evaluate the mass flux divergence term in (1):

$$\left(\frac{\partial M}{\partial x}\right)_m \approx \frac{1}{2}\left[\left(\frac{\partial M}{\partial x}\right)_m^{(n+1)} + \left(\frac{\partial M}{\partial x}\right)_m^{(n)}\right]$$

where n is the time step counter and m, the spatial grid point index. The time derivatives are centered on $n + 1/2$; a finite difference form of (1) can then be written:

$$h_m^{(n+1)} + \frac{1}{2}\Delta t\left(\frac{\partial M}{\partial x}\right)_m^{(n+1)} = h_m^{(n)} - \frac{1}{2}\Delta t\left(\frac{\partial M}{\partial x}\right)_m^{(n)} + A_m^{(n)}\Delta t - h'_m{}^{(n+1)} + h'_m{}^{(n)} \qquad \text{(B1)}$$

where Δt is the time step. The mass flux divergence at a grid point is calculated as the difference of mass flux leaving and entering a box of width Δx centered at the grid point. The ice sheet thickness at the boundaries of the box is taken as the mean of the adjacent grid point values.

To evaluate the nonlinear expression for the h on the left side in terms of the known terms on the right side of (B1), an iterative scheme based on the Newton-Raphson method is employed. This requires boundary conditions at each end of the domain of integration.

The north boundary point is taken as the point on the edge of the polar ocean; the south boundary point x_{SB} is taken as the first point beyond the ice sheet. The condition for the south boundary point is determined by requiring the mass flux out of the south side of its box to vanish. Predicted values of h_{SB} are saved, even when ice sheet thickness is negative, to be used in calculating the surface slope at the edge of the ice sheet. When the predicted value of ice sheet thickness at x_{SB} goes positive, the ice sheet is assumed to have advanced to the next grid point. This ad hoc procedure at the south boundary grid point was developed by trying many different schemes; it gives the most stable response, the smoothest growth and decay response, and the most realistic slopes near the leading edge. Except at x_{SB}, it is important to assure that spurious negative thicknesses do not appear in the extrapolation process.

For mass balance the net change in ice volume is

$$\frac{dV}{dt} = M_A - M_B - M_{SB} - M_{NB}$$

where V is the volume of the ice sheet, M_A is the mass added at the surface of the ice sheet in the accumulation zone, M_{AB} is the mass loss due to surface ablation, M_{NB} is the mass flux into the polar ocean, and M_{SB} is the mass flux due to the extension or retreat of the leading edge of the ice. Owing to the discretization in x, M_{SB} is generally not zero even in the steady state case.

An important criterion for model performance is that the grid spacing in x be sufficiently small so that, at least in times of slowly changing dimensions of the ablation zone, there will be several grid points in the ablation zone to give adequate estimates of M_{AB} relative to M_{SB}. If Δx is not small enough, it is not difficult to achieve a completely spurious steady state ice sheet with no ablation grid points, balance being achieved by large values of M_{SB} and M_{NB}.

The scheme for calculating the accumulation rate is modified in the region of the firn line, the latter being found by interpolation between grid points; the accumulation (positive or negative) at the grid point nearest the firn line is corrected for the presence of the firn line.

The most important features of the numerical scheme for its improved performance relative to earlier versions, are (1) the iteration scheme for handling the divergence of the mass flux, (2) sufficiently small finite difference interval to allow several grid points to fall in the ablation zone, (3) interpolation calculations near the firn line, and (4) the procedure for extrapolation of the leading edge of the ice sheet.

Acknowledgments. This research was supported by grant ATM8306251 from the Climate Dynamics Section, NSF. A great deal of appreciation is extended to those who reviewed an earlier version of this manuscript. In particular, we thank Michael Ghil not only for a most useful review but for several helpful conversations in regard to nonlinear oscillations and numerical methods of solution of nonlinear equations. We also express appreciation to T. Hughes, Isabelle Muszynski, and Albert Lunde for helpful conversations; the figures were drafted by Cheryl Cheverton.

REFERENCES

Berger, A., Long-term variations of daily insolation and Quaternary climatic changes, *J. Atmos. Sci.*, *35*, 2362–2367, 1978.

Birchfield, G. E., A study of the stability of a model continental ice sheet subject to periodic variations in heat input, *J. Geophys. Res.*, *82*, 4909–4913, 1977.

Birchfield, G. E., and J. Weertman, On long period internal oscillations in a simple ice sheet model, in *Milankovittich and Climate, Part II*, edited by A. L. Berger et al., pp. 605–606, D. Reidel, Hingham, Mass., 1978.

Birchfield, G. E., and J. Weertman, On long-period internal oscillations in a simple climate model with an ice sheet (abstract), *Ann. Glaciol.*, *5*, 200, 1984.

Birchfield, G. E., J. Weertman, and A. T. Lunde, A Pleistocene model of northern hemisphere ice sheets, *Quat. Res.*, *15*, 126–142, 1981.

Broecker, W. S., and J. Van Donk, Insolation changes, ice volumes, and the O^{18} record in deep-sea cores, *Rev. Geophys.*, *8*, 169–198, 1970.

Cathles, L. M., *The Viscosity of the Earth's Mantle*, Princeton University Press, Princeton, N. J., 1975.

Chen, W.-P., and P. Molnar, Focal Depths of intracontinental and intraplate earthquakes and their implications for the thermal and mechanical properties of the lithosphere, *J. Geophys. Res.*, *88*, 4183–4214, 1983.

Clark, S. P., Handbook of physical constants, *Mem. Geol. Soc. Am.*, *97*, 1966.

Daly, R. A., The changing world of the ice age, reprinted in *Glacial Isostacy*, edited J. T. Andrews, pp. 111–121, Dowden, Hutchinson and Ross, Stroudsburg, Pa., 1974.

Flint, R. F., *Glacial and Quaternary Geology*, John Wiley, New York, 1971.

Flint, R. F., and W. A. Gale, Glacial map of the United States east of the Rocky Mountains, scale 1:1,750,000, Geol. Soc. of Am., Boulder, Colo., 1959.

Ghil, M., and H. Le Treut, A climate model with cryodynamics and geodynamics, *J. Geophys. Res.*, *86*, 5262–5270, 1981.

Hays, J., J. Imbrie, and N. J. Shackleton, Variations in the earth's orbit: Pacemaker of the ice ages, *Sciences*, *194*, 1121–1132, 1976.

Hughes, T., Lithosphere deformation by continental ice sheets, *Proc. R. Soc. London, Ser. A*, *378*, 507–527, 1981.

Imbrie, J., A theoretical framework for the Pleistocene ice ages, *Q. J. Geol. Soc. London*, in press, 1985.

Imbrie, J., J. D. Hays, D. G. Martinson, A. McIntyre, A. C. Mix, J. J. Morley, N. G. Pisias, W. L. Prell, and N. J. Shackleton, The orbital theory of Pleistocene climate: Support from a revised chronology of the marine delta ^{18}O record, in *Milankovitch and Climate, Part I*, edited by A. L. Berger et al., pp. 269–305, D. Reidel, Hingham, Mass., 1984.

Kallen, E., C. Crafoord, and M. Ghil, Free oscillations in a climate model with ice sheet dynamics, *J. Atmos. Sci.*, *36*, 2292–2303, 1979.

Le Treut, H., and M. Ghil, Orbital forcing, climatic interactions and glaciation cycles, *J. Geophys. Res.*, *88*, 5167–5190, 1983.

Nicolet, C., Self-oscillations, external forcings, and climate predictability, in *Milankovitch and Climate, Part II*, edited by A. L. Berger et al., 637–653, D. Reidel, Hingham, Mass., 1984.

Oerlemans, J., Glacial cycles and ice sheet modelling, *Clim. Change*, *4*, 353–374, 1982.

Peltier, R., Dynamics of the ice age earth, *Adv. Geophys.*, *24*, 1–146, 1982.

Peltier, R., and W. Hyde, A model of the ice age cycle, in *Milankovitch and Climate, Part II*, edited by A. L. Berger et al., pp. 565–580, D. Reidel, Hingham, Mass., 1984.

Pollard, D., A coupled climate–ice sheet model applied to the Quaternary ice ages, *J. Geophys. Res.*, *88*, 7705–7718, 1983.

Pollard, D., Some ice-age aspects of a calving ice-sheet model, in *Milankovitch and Climate, Part II*, edited by A. L. Berger et al., pp. 541–564, D. Reidel, Hingham, Mass., 1984.

Saltzman, B., and A. R. Sutera, A model of the internal feedback system involved in late Quaternary climatic variations, *J. Atmos. Sci.*, *41*, 736–745, 1984.

Saltzman, B., A. Sutera, and A. Evenson, Structural stochastic stability of a simple auto-oscillatory climatic feedback system, *J. Atmos. Sci.*, *38*, 494–503, 1981.

Saltzman, B., A. Sutera, and A. R. Hansen, A possible marine mechanism for internally generated long-period climate cycles, *J. Atmos. Sci.*, *39*, 2634–2637, 1982.

Saltzman, B., A. Sutera, and A. R. Hansen, Long period free oscillations in a three-component climate model, in *New Perspectives in Climate Modelling*, edited by A. L. Berger and C. Nicolis, pp. 289–298, Elsevier, New York, 1984.

Saltzman, B., A. R. Hansen, and K. A. Maasch, The late Quarternary glaciations as the response of a three-component feedback system to earth-orbital forcing, *J. Atmos. Sci.*, in press, 1985.

Shackleton, N. J., and N. D. Opdyke, Oxygen isotope and paleomagnetic stratigraphy of equatorial Pacific core V28-238: Oxygen isotope temperatures and ice volumes on a 10^5 year and 10^6 year scale, *Quat. Res.*, *3*, 39–55, 1973.

Sibson, R. H., Fault zone models, heat flow and the depth distribution of earthquakes in the continental crust of the United States, *Bull. Seismol. Soc. Am.*, *72*, 151–163, 1982.

Turcotte, D. L., and G. Schubert, *Geodynamics*, John Wiley, New York, 1982.

Uyeda, S., *The New View of the Earth*, W. H. Freeman, San Francisco, Calif., 1978.

Weertman, J., Creep laws for the mantle of the earth, *Philos. Trans. R. Soc. London, Ser. A*, *288*, 9–26, 1978.

Wiens, D. A., and S. Stein, Age dependence of oceanic intraplate seismicity and implications for lithospheric evolution, *J. Geophys. Res.*, *88*, 6455–6468, 1983.

Wigley, T. M. L., Spectral analysis and the astronomical theory of climatic change, *Nature*, *264*, 629–631, 1976.

G. E. Birchfield and R. W. Grumbine, Department of Geological Sciences, Locy Hall, Northwestern University, Evanston, IL 60201.

(Received December 26, 1984;
revised June 13, 1985;
accepted June 26, 1985.)